HHS Public Access

Author manuscript

J Magn Reson Imaging. Author manuscript; available in PMC 2018 February 01.

Published in final edited form as:

J Magn Reson Imaging. 2017 February ; 45(2): 472–481. doi:10.1002/jmri.25367.

Effects of Arterial Transit Delay on Cerebral Blood Flow Quantification using Arterial Spin Labeling in an Elderly Cohort

Weiying Dai[1,2], **Tamara Fong**[3], **Richard N. Jones**[4], **Edward Marcantonio**[5], **Eva Schmitt**[6], **Sharon K. Inouye**[6,7], and **David C. Alsop**[1]

[1]Department of Radiology, Beth Israel Deaconess Medical Center and Harvard Medical School, Boston, MA

[2]Department of Computer Science, State University of New York at Binghamton, Binghamton, NY

[3]Department of Neurology, Beth Israel Deaconess Medical Center and Harvard Medical School, Boston, MA

[4]Department of Psychiatry and Human Behavior and Neurology, Warren Alpert Medical School, Brown University, Providence, RI

[5]Department of Medicine, Beth Israel Deaconess Medical Center and Harvard Medical School, Boston, MA

[6]Institute for Aging Research, Hebrew SeniorLife, Boston, MA

[7]Department of Gerontology, Beth Israel Deaconess Medical Center and Harvard Medical School, Boston, MA

Abstract

Purpose—This study is to investigate whether measurement of arterial transit time (ATT) can improve the accuracy of Arterial Spin Labeling (ASL) cerebral blood flow (CBF) quantification in an elderly cohort due to the potentially prolonged ATT in the cohort.

Methods—We employed a 1 minute, low resolution (12 mm in plane), sequential multi-delay ATT measurement (both with and without vessel suppression) approach to characterize and correct ATT errors in CBF imaging of an elderly, clinical cohort. 140 non-demented subjects greater than 70 years old were imaged at 3 Tesla with a single delay, volumetric continuous ASL sequence and also with the fast ATT measurement method. 9 healthy young subjects (28 ± 6 years old) were also imaged.

Results—ATT's measured without vessel suppression (superior frontal: 1.51 ± 0.27s) in the elderly were significantly shorter than those with suppression ($p<0.0001$). Correction of CBF for ATT significantly increased average CBF in multiple brain regions where ATT was longer than the post-labeling delay ($p < 0.01$) and decreased inter-subject variability of CBF in frontal, parietal, and occipital regions ($p < 10^{-8}$). Measured ATT with vessel suppression was significantly longer in the elderly subjects (e.g. superior frontal: 1.76 ± 0.25s) compared to the younger adults (superior frontal: 1.59 ± 0.19s) in basal ganglia and frontal cortical regions ($p < 0.05$).

Conclusions—The ATT measurement is beneficial for imaging of elderly clinical populations. If ATT mapping is not feasible or available, post-labeling delays of 2–2.3s should be used for elderly populations based on longest measured regional ATTs.

Keywords

Arterial Spin labeling; cerebral blood flow; arterial transit time; elderly cohort; magnetic resonance imaging

INTRODUCTION

Arterial spin labeling (ASL) is a completely noninvasive magnetic resonance imaging (MRI) technique capable of quantifying regional cerebral blood flow (CBF)(1–3). ASL has been adopted to study a broad range of clinical disorders and has shown disease specific CBF changes (see reviews (4,5)). Though validated in younger subjects, CBF measurement with ASL may still suffer from systematic errors in clinical cohorts where age and disease can alter blood flow dynamics. A major concern for using ASL in elderly populations is the potentially slower transit from the labeling location to arrival in brain tissue caused by age-related alterations of brain vasculature such as increased vessel tortuosity(6–8). Failure to account for this longer Arterial Transit Time (ATT) may compromise the accuracy of the CBF measurement and mask or confuse the interpretation of normal aging or pathologic alterations of CBF.

Relatively few ASL CBF studies have been reported in subjects older than 70 and even fewer have examined ATT effects. Most studies in the elderly have used a single post-labeling delay after labeling and assumed the delay is longer than the ATTs for the whole brain (e.g. the Alzheimer's disease studies in the review (9)). Several ASL studies have reported age related gray matter CBF reductions but are limited by using a broad age range with only a small proportion of subjects over age 70 (10–13). In these studies, uncertainty in ATT may combine with issues of subject exclusion for comorbidities to introduce variance across studies in the slope of the age effects. ATTs have been reported to increase with advancing age (10,14). Two pulsed ASL studies have reported increased ATT in older subjects relative to younger subjects: one studied the age effects in ATT but mostly in subjects below 70 years of age (10) and the other one reported optimized parameters for pulsed ASL in their "elderly" group who were age 61–67 years old (14). Pulsed ASL techniques have been used to measure several hemodynamic parameters including a measure of ATT and have been applied to comparisons of Alzheimer's disease groups with matched elderly controls (15,16). Recently a flow dephasing continuous ASL approach(17) has been used to characterize transit times and their variability in an elderly cohort with hypertension(18).

A number of strategies for measuring ATT have been reported. All of them in some way lengthen or degrade the signal-to-noise ratio (SNR) of the blood flow measurement. ATT varies strongly across different brain regions (16,19–21) and therefore regional or voxel-based ATT mapping is necessary to accurately measure ATT effects. ATT mapping requires acquiring two or more images with different labeling timing, different gradient suppression of vascular signal (17), or both (22–25). ATT measured without vascular suppression is shorter because blood need only reach larger vessels in the voxel rather than pass all the way through the microvasculature and into the tissue. If the vessels are large enough to flow back

out of the voxel, however, the ATT can be inaccurate and will underestimate the tissue arrival time. When a substantial number of different labeling delays are used to enable measurement of a wide range of ATT's, degradation of SNR is substantial, but can be minimized by Hadamard time encoding of the labeling (26–28). Another strategy to minimize the SNR and scan time penalties is to reduce the resolution of the imaging for the ATT measurement, which reduces the additional time required (19).

The impact of longer ATT's on ASL CBF studies in elderly subjects and the best strategies to minimize them have not been fully investigated. Therefore, the primary goal of this study was to investigate whether the ATT measurement in the elderly can increase the CBF quantification accuracy and reduce the variance of CBF. The secondary goal of this study was to explore whether the elderly had longer ATT compared to the young. In addition, we have explored the effect of vessel suppression on ATT measurements because it has not been studied rigorously regarding its advantages or disadvantages when applied to ATT measurements. In the study, ATT maps with and without vessel suppression, were measured using the recently proposed quick and low-resolution ATT methods (19) in an elderly, presurgical cohort.

METHODS

Subjects

One hundred and forty elderly subjects (57 males and 83 females, 70–95 years old with 76 +/−4.45 years) were studied with the ATT mapping and ASL imaging sequences. The subjects were part of the Successful Aging after Elective Surgery (SAGES) cohort study, an ongoing prospective cohort study of older adults undergoing major elective surgery. The study design and methods have been described in detail previously (29). In brief, eligible participants were age 70 years and older, English speaking and able to communicate verbally, scheduled to undergo elective surgery at two academic medical centers with an anticipated length of stay of at least 3 days, and available for in-person follow-up interviews. Subjects older than 70 are at disproportionate risk for dementia (30) and stroke (31) and many other age-related disorders, including post-surgical delirium (32). Eligible surgical procedures were: total hip or knee replacement, lumbar, cervical, or sacral laminectomy, lower extremity arterial bypass surgery, open abdominal aortic aneurysm repair, and open or laparoscopic colectomy. Exclusion criteria included evidence of dementia, delirium, prior hospitalization within 3 months, legal blindness, severe deafness, terminal condition, history of schizophrenia or psychosis, and history of alcohol abuse or withdrawal. A total of 566 patients met all eligibility criteria and were enrolled between June 18, 2010 and August 8, 2013.

A subset of approximately one-third of the enrolled SAGES study participants was recruited to undergo MRI one month prior to surgery (n=147). Additional exclusion criteria for the nested cohort MRI study included contraindications to 3 Tesla MRI (such as pacemakers, and certain stents and implants). Of the MRI cohort, only 140 subjects were studied after the ATT sequence was added to the protocol and the presurgical scans from these subjects are reported here. The entire MRI substudy including image acquisitions and analysis were approved as part of the overall study IRB. An additional written informed consent for study

participation was obtained from all participants in the MRI substudy according to procedures approved by the institutional review boards of Beth Israel Deaconess Medical Center and Brigham and Womens's Hospital, the two study hospitals, and Hebrew SeniorLife, the study coordinating center, all located in Boston.

Nine young healthy subjects (6 males and 3 females, 21–40 years old with 27.9±6.3 years old) were studied with the ATT mapping from a previous study (19). The young subjects were included for comparison purpose between the elderly and the young regarding their spatial distribution of the ATT map and regional ATT values.

In vivo Measurements

All 140 elderly subjects were scanned on the same GE 3.0 Tesla HDxt scanner using the receive-only 8-channel head array coil and the body transmit coil. Each subject was scanned following an identical CBF imaging protocol: Pseudo-continuous arterial spin labeling (PCASL) (33) was used for CBF acquisition with 3.5 s labeling and 1.5 s post-labeling delay. An additional reference image was appended after the ASL sequence to provide necessary M_0 values for quantification. A low-resolution transit time acquisition with labeling duration of 2 s and five post-labeling delays of 0.7 s, 1.3 s, 1.9 s, 2.5 s, 3.0 s was performed both with vessel suppression (34) and without vessel suppression. T1 images were acquired with a 3D modified driven equilibrium Fourier transform (MDEFT) sequence (TR of 7.9 ms, a TE of 3.2 ms, a 15° flip angle and 32 kHz bandwidth, a coronal acquisition plane with 24×19 cm field of view, 0.94 mm in plane resolution, 1.4 mm slices, a preparation time of 1100 ms with repeated saturation at the beginning of the preparation period, and an adiabatic inversion pulse 500 ms before imaging).

Nine young healthy subjects were scanned using the same low-resolution ATT acquisition sequence (same labeling duration of 2 s and five post-labeling delays) as the elderly subjects. The ATT acquisitions were from a previous study (19) and scanned with vessel suppression only. Therefore, the vessel-suppressed ATTs from the elderly subjects were used to compare with those obtained from the young subjects.

All ASL and reference images were acquired with a 3D stack of spirals RARE imaging sequence (33,35). Each preparation sequence was followed by a 90° excitation pulse and then a series of 44 spin echoes encoded with the same spiral gradient but different slice encoding phase encode gradients. 44 slices of nominally 4 mm thickness were encoded with a centric phase encode order. The resolution was determined by the number of spiral interleaves selected. The ASL and low-resolution ATT acquisitions used 8 spiral interleaves and 1 spiral interleave, producing an estimated spatial resolution of 3.07 mm and 12.08 mm respectively.

Image Analysis

ATT maps were derived voxel-by-voxel by applying a non-iterative algorithm to the ASL data with five post-labeling delays (19). Compared to an iterative algorithm for fitting the ASL signal as a function of five different post-labeling delays, the non-iterative algorithm provides more robust analytical solution by taking advantage of the monotonic relationship between transit time and signal weighted post-labeling delay. CBF maps were calculated

both with a standard quantification method without ATT correction and the method with ATT correction (19) using the one-compartment CBF kinetic model (22, 36–37), Eq. [1]. For the standard quantification method, the applied post-labeling delay of 1.5 s is assumed to be same as the ATT in the entire brain. For the method with ATT correction, the perfusion map was calculated with the derived low-resolution ATT map according to the equation.

$$\Delta M = 2M_t^0 \cdot \beta \cdot \alpha \cdot T_{1t} \cdot f \cdot e^{-\frac{\delta}{T_{1a}}} \cdot \frac{e^{-\frac{\max(w-\delta,0)}{T_{1t}}} - e^{-\frac{\max(\tau+w-\delta,0)}{T_{1t}}}}{\lambda} \quad [1]$$

where ΔM is the PCASL difference signal, f is the perfusion rate, and T_{1a} and T_{1t} are the longitudinal relaxation times of blood and tissue (assumed to be 1.66s (38) and 1.5s (39) respectively),. M_t^0 is the fully relaxed equilibrium magnetization of brain tissue, α is the efficiency of the labeling sequence (assumed to be 0.8 (33)), λ is the tissue-to-blood partition coefficient of water (assumed to be 0.9 ml of blood/g of tissue (40)), δ is the transit time, τ is the labeling duration and w is the post-labeling delay. Suppression of vascular signals is assumed in this model. β is any static tissue signal loss caused by the vessel suppression pulses (β = 1 because no vessel suppression was applied for the PCASL perfusion sequence).

For each subject, the CBF maps were normalized to the a priori gray matter template of SPM8 (http://www.fil.ion.ucl.ac.uk/spm/). To allow for better alignment with the template, T1 images, which can provide the detailed structural information, were used for the normalization. T1 images were first segmented by the “new segment” algorithm (41) in SPM8, which output gray matter images and other images in the original image space. The subtraction images (between label and control) were co-registered to gray matter images and the gray matter images were normalized to the gray matter template in SPM8. The combined warping parameters from the coregistration and normalization were used to warp the quantitative CBF maps and the transit time maps from that subject to the SPM8 template space. Quantitative CBF maps were smoothed using a Gaussian kernel with full-width at half maximum (FWHM) of 8 mm, and transit time maps were not smoothed further because the maps have low spatial resolution of 12 mm. Voxel-based statistical analyses were performed to compare the ATT maps with/without vessel suppression and a fixed delay of 1.5 s using a one-sample t test. To investigate the effect of the ATT on CBF, CBF maps with correction using the ATT maps were compared with those without ATT correction using a paired t test. Both tests were thresholded with voxel-level p value of 0.01 and multiple-comparison corrected with cluster-level threshold of P = 0.01.

The MNI Automated Anatomical Labeling (AAL) atlas (42) was used to generate regional masks for the following regions of interest: superior, middle and inferior regions of frontal, temporal, and occipital cortex, superior and inferior regions of parietal cortex and basal ganglia. Each anatomical mask was projected onto the ATT map to calculate the average transit times.

Paired t tests were used to compare the regional ATT difference of the elderly cohort between with and without vessel suppression. Mann-Whitney U-tests were used to compare the regional vessel-suppressed ATT difference between the elderly and the young subjects ($p < 0.05$). Mann-Whitney U-tests instead of two-sample t tests were used because the smaller number of young subjects might make results more sensitive to violation of the normality assumption. To evaluate the regional ATT distributions in the elderly subjects, histograms of ATT values were plotted for all the cortical regions and basal ganglia. Jarque-Bera tests were performed to test for whether the ATT values from the regions come from a normal distribution. In addition, skewness values were also calculated to show the tendency of asymmetry for each regional ATT values.

Our hypothesis is that CBF variability across subjects would be reduced after the ATT correction if the ATT correction is beneficial to the CBF measurement. Therefore, CBF variability across subjects was compared between the CBF maps without and with ATT corrections. CBF variability was defined as the coefficient of variation (CV = standard deviation/mean) map across subjects. Standard deviation and mean maps were calculated across subjects for the CBF maps with and without ATT correction. The effect of ATT correction on CBF variability was then tested using Pitman's t tests (43–45). Pitman's t tests were used instead of F tests because the CBF maps are from the same subjects and are therefore correlated. Pitman's t tests were performed on both the region with reduced and the region with increased CBF variability. All the region-wise statistical tests were performed using MATLAB 8.5 (The MathWorks Inc., Natick, MA).

RESULTS

All subjects successfully completed the low resolution ATT mapping and higher resolution CBF scans. Demographic variables for the subject groups are tabulated in table 1. Example multi-delay and ATT images results from a representative subject are shown in Fig. 1.

Consistent with prior studies with young subjects, ATT in the elderly varied considerably across brain regions (Fig. 2a). The spatial pattern was similar for elderly and young subjects (Fig. 2), although younger subjects had significantly shorter transit times (Mann-Whitney tests with $p < 0.05$) for all the frontal regions and the basal ganglia (Table 2). Specifically, Mann-Whitney two-tailed tests showed the significantly different ATT values between the elderly and the young for the superior frontal ($p = 0.031$), middle frontal ($p = 0.029$), inferior frontal ($p = 0.017$), and basal ganglia ($p = 0.0019$) regions. Generally, shorter delays were measured in the center of major artery territories with longer delays in the borderzone regions. Delays to the basal ganglia were the shortest of any region in the brain. Although some subjects demonstrated somewhat altered spatial distributions, the stereotypical spatial distribution was apparent in all individual subject scans, regardless of age.

ATT values of the elderly subjects were substantially larger in the vessel suppressed images than the unsuppressed images (Fig. 1). ATT values were significantly longer ($p<0.0001$) for all investigated brain regions with vessel suppression than without, with most regions showing approximately 300 ms longer ATT with vessel suppression.

ATT values were often substantially longer than the 1.5 s assumed by our selection of post-labeling delay for the CBF imaging. To better display the frequency with which a delay of 1.5 s was exceeded, histograms of ATT values, with vessel suppression and without vessel suppression, were plotted across all subjects for all the cortical regions and basal ganglia (Fig. 3a and Fig. 3b). The ATT histograms suggest a non-Gaussian distribution, especially for the vessel-suppressed ATT histograms, and appeared to skew to the higher ATT values for except in the basal ganglia region. The frontal, occipital, parietal, and temporal regions showed negative skewness values of −0.38, −0.79, −0.46 and −0.27 respectively while basal ganglia showed positive skewness value of 0.45, which is consistent with the asymmetry tendency for the visual appearance of the regional ATT distributions in the elderly. However, only the ATT values at the occipital region and basal ganglia region followed non-Gaussian distribution according to the Jarque-Bera tests ($p < 0.05$). Although similar ATT ranges were observed in all regions between without vessel suppression and with vessel suppression, the centers of the distributions shifted to the right, which confirms the longer ATT values in the vessel-suppressed images. In the frontal, occipital, parietal, temporal and basal ganglia regions respectively, 35.00%, 77.14%, 67.14%, 28.57%, 9.29% of subjects have non-vessel-suppressed regional ATTs longer than 1.5s, while 78.57%, 97.14%, 95.71%, 73.57%, 22.14% of subjects have vessel-suppressed ATTs longer than 1.5s.

CBF increased after ATT correction in most regions, and especially in parietal and occipital regions (Fig. 4a). Regions with CBF increase upon correction are consistent with those where ATTs were longer than the applied post-labeling delay of 1.5s (Fig. 4b). This confirms that without ATT maps, CBF was systematically underestimated in the regions with significantly longer ATT values (corrected $p<0.01$). The ATT was significantly shorter than 1.5 s in only the basal ganglia region on the ATT maps with vessel suppression (corrected $p<0.01$), Fig. 4c. Without vessel suppression, ATT was underestimated around the circle of Willis, where large vessels contaminate the ATT estimate, Fig. 4d. Therefore, the accuracy of CBF measurement using the non-vessel-suppressed ATT maps will be compromised in regions with large vessels. Because the regions with large arterial vessels tend to have short ATT anyway and there is little effect from underestimation of ATT as long as the true ATT is shorter than the post-labeling, the effect of ATT underestimation on the accuracy of flow quantification is expected to be small (Fig. 4a).

With ATT correction, CBF variability across subjects was reduced in frontal regions and even more in parietal and occipital regions, but was increased in the cerebellum and pons regions (Fig. 5). Both the region with reduced and the region with increased CBF variability were chosen as masks on the CBF variability map with a threshold shown on Fig. 4, corresponding to the regions with red-yellow color or green color. CBF variability decrease was significant ($p<10^{-8}$) but the increased variability was not significant ($p = 0.43$). These results indicate that ATT measurement can improve the reliability and accuracy of CBF measurement in elderly populations.

DISCUSSION

We have shown the feasibility of the vessel suppressed and non-vessel suppressed ATT mapping methods in elderly populations. Multi-delay low resolution ATT mapping

sequences were sufficient to quantify ATT in subjects as old as 95 years old. ATT values measured with both methods are heterogeneous across different brain regions but vessel suppressed ATT values are significantly longer than non-vessel suppressed ATT values. This is consistent with the longer time required for blood to reach smaller vessels or tissue rather than higher up in the vascular supply. Compared to the young, vessel-suppressed ATT values in the elderly are significantly longer in the frontal regions and basal ganglia. Cortical vessel-suppressed ATT values in the elderly have broader but more skewed distribution to long ATT values. The more skewed distribution ATT values in the elderly suggests that transit times do not uniformly increase with age but rather a fraction of subjects have a substantial increase, perhaps reflecting the distribution of cerebrovascular disease or other ATT modifying factor in the population.

In this study, non-vessel suppressed ATT maps were used to correct the CBF difference maps because the ASL images were acquired without vessel suppression. However, it is preferable to acquire the ASL images with vessel suppression to minimize the intravascular signals. As shown in the study, non-vessel suppressed ATT values were underestimated in regions with large vessels and therefore using the ATT values should cause small but systematic error to CBF measurement. To avoid the systematic error, it is generally preferable to obtain vessel suppressed ATT maps and vessel suppressed ASL CBF difference images. It is worth noting that the vessel suppression sequence may cause some static tissue signal loss. If the vessel suppression sequence is performed before the ASL acquisition, the vessel suppression should preferably be performed before the reference image acquisition also so they should have a comparable attenuation. Hence CBF quantification will be accurate because the static tissue signal loss with the vessel suppression preparation, β in Eq. [1], cancels out upon division by the reference image. Quantification of vessel suppressed ATT map will still be accurate because the static tissue signal loss factor β also cancels out due to ASL signals at different post-labeling delays appearing both on the denominator and numerator of ATT calculation formula (19).

Our study bears similarities to the recent study of Mutsaerts et al.(18) that used a gradient dephasing approach to estimate ATT in an elderly cohort with hypertension. Qualitatively similar spatial distributions of transit time were observed and some improvement in coefficient of variation was observed with ATT correction. The flow encoding arterial spin tagging (FEAST) technique (17) used in that study requires that all ATT's without vessel suppression be shorter than the post-labeling delay and all ATT's with vessel suppression be longer than the post-labeling delay. With their selected post-labeling delay of 1.5–1.9 s, shorter transit times such as in the basal ganglia could not be measured. Indeed, our results suggest that no post-labeling delay precisely meets this criterion across regions and subjects. Continued innovation in ATT transit time measurement and correction methods suggests both our method and that of Mutsaerts et al. will be improved in future studies, but the qualitative conclusions regarding ATT and its contribution to variation in studies of elderly cohorts will likely be confirmed.

We have shown that ATT measurement can decrease the CBF variability in frontal regions and even more in parietal and occipital regions. The regional distribution is consistent with the distribution of ATT, i.e. the regions with longer ATTs have lower precision and accuracy

than regions with shorter ATT's. The mean CV across the whole brain pixels decreased 10.17% with the ATT correction compared to without the ATT correction. When performing cross-sectional group comparisons, CBF maps are frequently normalized by global CBF to reduce the cross-subject variations (46,47). We therefore compared the CBF variability without and with ATT correction after global normalization (divided by the mean CBF over the brain mask). Reduced CBF variability was no longer observed in the regions with longer ATTs, which suggests that global normalization diminishes the need for ATT correction. If the change of absolute CBF is not of interest, obtaining an extra ATT map may not be necessary for cross-sectional group comparison. To more accurately estimate the regional CBFs for all the elderly subjects without transit time mapping, the post-labeling delay should be set to the maximum ATT values across the regions and the subjects: 2.31s without vessel suppression and 2.36s with vessel suppression. This will assure that the post-labeling delay is longer than the transit times for all regions and subjects, a necessary condition for accurate CBF quantification without individual subject ATT mapping (22). Consistent with recent consensus guidelines (35), we suggest using a longer post-labeling delay (between 2–2.3s) in elderly cohorts to reduce the sensitivity to ATT when ATT mapping is unavailable or too time consuming.

We have compared the regional ATT difference between the elderly subjects and the young subjects and shown significant longer ATT values for the elderly in the frontal regions and basal ganglia region compared to the young using nonparametric statistical comparison. Although gender distributions are not well matched between the two groups, it does not invalidate the findings of significantly longer ATT values for the elderly relative to the young in certain regions. We have compared regional ATT values between the female and male group in the elderly group and found that females have significant shorter ATT values than males for all the investigated regions, which is consistent with the literature (10). With a matched gender distribution in the young group, we would expect to obtain even shorter ATT values for the young group in the frontal regions and basal ganglia region and thus more regional ATT difference between the young and elderly groups for the regions.

Our study is not without limitations. First, the number of subjects in the young group is small and therefore some comparison results between the young and the elderly may not generalize well. For example, the unobserved ATT differences between the young and elderly in the temporal, parietal and occipital regions may be obscured by unmatched gender distribution between the two age groups. Second, some of the elderly patients may still have co-morbid vascular conditions although we have tried to limit the vascular conditions known by the patients, and therefore we could not completely rule out the ATT difference partially caused by vascular co-morbidities We consider the changes to be age associated but the association may well be mediated by age associated pathology rather than normal aging.

We have shown the feasibility of the ATT mapping methods with and without vessel suppression in an elderly clinical population. Measured ATT was significantly longer in the elderly subjects compared to younger adults in basal ganglia and frontal cortical regions. ATT's measured without vessel suppression were significantly shorter than those with suppression, but suffered from underestimation of ATT near major vessels. Correction of CBF for ATT significantly increased average CBF in multiple brain regions where ATT was

longer than the post-labeling delay and decreased inter-subject variability of CBF in frontal, parietal, and occipital regions.

We especially recommend the ATT correction when absolute CBF is of interest: such as in cross-sectional analyses if change in absolute CBF is of interest, in longitudinal analyses when change over time is of interest, or in regional analysis when the absolute CBF of certain regions (e.g. frontal, parietal, and occipital regions which are more affected by ATT variability) is of interest. If ATT mapping is not available, post-labeling delays of 2–2.3s should be used in broad elderly populations.

Acknowledgments

This work was supported in part by Grants No. P01AG031720 (SKI) and K07AG041835 (SKI) from the National Institute on Aging and Grant No, R01MH080729 (DCA) from the National Institute of Mental Health. Dr. Inouye holds the Milton and Shirley F. Levy Family Chair. The funding sources had no role in the design, conduct, or reporting of this study.

References

1. Detre JA, Leigh JS, Williams DS, Koretsky AP. Perfusion imaging. Magn Reson Med. 1992; 23(1): 37–45. [PubMed: 1734182]
2. Detre JA, Zhang W, Roberts DA, Silva AC, Williams DS, Grandis DJ, Koretsky AP, Leigh JS. Tissue specific perfusion imaging using arterial spin labeling. NMR Biomed. 1994; 7(1–2):75–82. [PubMed: 8068529]
3. Williams DS, Detre JA, Leigh JS, Koretsky AP. Magnetic resonance imaging of perfusion using spin inversion of arterial water. Proc Natl Acad Sci U S A. 1992; 89(1):212–216. [PubMed: 1729691]
4. Brown GG, Clark C, Liu TT. Measurement of cerebral perfusion with arterial spin labeling: Part 2. Applications J Int Neuropsychol Soc. 2007; 13(3):526–538. [PubMed: 17445302]
5. Detre JA, Alsop DC. Perfusion magnetic resonance imaging with continuous arterial spin labeling: methods and clinical applications in the central nervous system. Eur J Radiol. 1999; 30(2):115–124. [PubMed: 10401592]
6. Farkas E, Luiten PG. Cerebral microvascular pathology in aging and Alzheimer's disease. Prog Neurobiol. 2001; 64(6):575–611. [PubMed: 11311463]
7. Hutchins PM, Lynch CD, Cooney PT, Curseen KA. The microcirculation in experimental hypertension and aging. Cardiovasc Res. 1996; 32(4):772–780. [PubMed: 8915195]
8. Sonntag WE, Lynch CD, Cooney PT, Hutchins PM. Decreases in cerebral microvasculature with age are associated with the decline in growth hormone and insulin-like growth factor 1. Endocrinology. 1997; 138(8):3515–3520. [PubMed: 9231806]
9. Alsop DC, Dai W, Grossman M, Detre JA. Arterial spin labeling blood flow MRI: its role in the early characterization of Alzheimer's disease. J Alzheimers Dis. 2010; 20(3):871–880. [PubMed: 20413865]
10. Liu Y, Zhu X, Feinberg D, Guenther M, Gregori J, Weiner MW, Schuff N. Arterial spin labeling MRI study of age and gender effects on brain perfusion hemodynamics. Magn Reson Med. 2012; 68(3):912–922. [PubMed: 22139957]
11. Biagi L, Abbruzzese A, Bianchi MC, Alsop DC, Del Guerra A, Tosetti M. Age dependence of cerebral perfusion assessed by magnetic resonance continuous arterial spin labeling. J Magn Reson Imaging. 2007; 25(4):696–702. [PubMed: 17279531]
12. Parkes LM, Rashid W, Chard DT, Tofts PS. Normal cerebral perfusion measurements using arterial spin labeling: reproducibility, stability, and age and gender effects. Magnetic Resonance in Medicine. 2004; 51(4):736–743. [PubMed: 15065246]
13. Chen JJ, Rosas HD, Salat DH. The relationship between cortical blood flow and sub-cortical white-matter health across the adult age span. PLoS One. 2013; 8(2):e56733. [PubMed: 23437228]

14. Campbell AM, Beaulieu C. Pulsed arterial spin labeling parameter optimization for an elderly population. Journal of magnetic resonance imaging : JMRI. 2006; 23(3):398–403. [PubMed: 16463300]
15. Mak HK, Chan Q, Zhang Z, Petersen ET, Qiu D, Zhang L, Yau KK, Chu LW, Golay X. Quantitative assessment of cerebral hemodynamic parameters by QUASAR arterial spin labeling in Alzheimer's disease and cognitively normal Elderly adults at 3-tesla. J Alzheimers Dis. 2012; 31(1):33–44. [PubMed: 22504315]
16. Yoshiura T, Hiwatashi A, Yamashita K, Ohyagi Y, Monji A, Takayama Y, Nagao E, Kamano H, Noguchi T, Honda H. Simultaneous measurement of arterial transit time, arterial blood volume, and cerebral blood flow using arterial spin-labeling in patients with Alzheimer disease. AJNR Am J Neuroradiol. 2009; 30(7):1388–1393. [PubMed: 19342545]
17. Wang J, Alsop DC, Song HK, Maldjian JA, Tang K, Salvucci AE, Detre JA. Arterial transit time imaging with flow encoding arterial spin tagging (FEAST). Magn Reson Med. 2003; 50(3):599–607. [PubMed: 12939768]
18. Mutsaerts HJ, van Dalen JW, Heijtel DF, Groot PF, Majoie CB, Petersen ET, Richard E, Nederveen AJ. Cerebral Perfusion Measurements in Elderly with Hypertension Using Arterial Spin Labeling. PLoS One. 2015; 10(8):e0133717. [PubMed: 26241897]
19. Dai W, Robson PM, Shankaranarayanan A, Alsop DC. Reduced resolution transit delay prescan for quantitative continuous arterial spin labeling perfusion imaging. Magn Reson Med. 2012; 67(5): 1252–1265. [PubMed: 22084006]
20. Qiu M, Paul Maguire R, Arora J, Planeta-Wilson B, Weinzimmer D, Wang J, Wang Y, Kim H, Rajeevan N, Huang Y, Carson RE, Constable RT. Arterial transit time effects in pulsed arterial spin labeling CBF mapping: insight from a PET and MR study in normal human subjects. Magn Reson Med. 2010; 63(2):374–384. [PubMed: 19953506]
21. MacIntosh BJ, Filippini N, Chappell MA, Woolrich MW, Mackay CE, Jezzard P. Assessment of arterial arrival times derived from multiple inversion time pulsed arterial spin labeling MRI. Magn Reson Med. 2010; 63(3):641–647. [PubMed: 20146233]
22. Alsop DC, Detre JA. Reduced transit-time sensitivity in noninvasive magnetic resonance imaging of human cerebral blood flow. J Cereb Blood Flow Metab. 1996; 16(6):1236–1249. [PubMed: 8898697]
23. Gunther M, Bock M, Schad LR. Arterial spin labeling in combination with a look-locker sampling strategy: inflow turbo-sampling EPI-FAIR (ITS-FAIR). Magn Reson Med. 2001; 46(5):974–984. [PubMed: 11675650]
24. Gonzalez-At JB, Alsop DC, Detre JA. Cerebral perfusion and arterial transit time changes during task activation determined with continuous arterial spin labeling. Magn Reson Med. 2000; 43(5): 739–746. [PubMed: 10800040]
25. Petersen ET, Lim T, Golay X. Model-free arterial spin labeling quantification approach for perfusion MRI. Magn Reson Med. 2006; 55(2):219–232. [PubMed: 16416430]
26. Dai W, Shankaranarayanan A, Alsop DC. Volumetric measurement of perfusion and arterial transit delay using hadamard encoded continuous arterial spin labeling. Magn Reson Med. 2013; 69(4): 1014–1022. [PubMed: 22618894]
27. Wells JA, Lythgoe MF, Gadian DG, Ordidge RJ, Thomas DL. In vivo Hadamard encoded continuous arterial spin labeling (H-CASL). Magn Reson Med. 2010; 63(4):1111–1118. [PubMed: 20373414]
28. Guenther, M. Highly efficient accelerated acquisition of perfusion inflow series by Cycled Arterial Spin Labeling. Berlin: 2007. p. 380
29. Schmitt EM, Marcantonio ER, Alsop DC, Jones RN, Rogers SO Jr, Fong TG, Metzger E, Inouye SK, Group SS. Novel risk markers and long-term outcomes of delirium: the successful aging after elective surgery (SAGES) study design and methods. J Am Med Dir Assoc. 2012; 13(9):818 e811–810.
30. Ott A, Breteler MM, van Harskamp F, Stijnen T, Hofman A. Incidence and risk of dementia. The Rotterdam Study. Am J Epidemiol. 1998; 147(6):574–580. [PubMed: 9521184]
31. Wolf PA, D'Agostino RB, Belanger AJ, Kannel WB. Probability of stroke: a risk profile from the Framingham Study. Stroke. 1991; 22(3):312–318. [PubMed: 2003301]

32. Fong TG, Tulebaev SR, Inouye SK. Delirium in elderly adults: diagnosis, prevention and treatment. Nat Rev Neurol. 2009; 5(4):210–220. [PubMed: 19347026]
33. Dai W, Garcia D, de Bazelaire C, Alsop DC. Continuous flow-driven inversion for arterial spin labeling using pulsed radio frequency and gradient fields. Magn Reson Med. 2008; 60(6):1488–1497. [PubMed: 19025913]
34. Dai, W.; Robson, PM.; Shankaranarayanan, A.; Alsop, DC. Optimization and Implementation of Vessel Suppression Preparation for ASL MRI 2009. Honolulu: p. 1512
35. Alsop DC, Detre JA, Golay X, Gunther M, Hendrikse J, Hernandez-Garcia L, Lu H, Macintosh BJ, Parkes LM, Smits M, van Osch MJ, Wang DJ, Wong EC, Zaharchuk G. Recommended implementation of arterial spin-labeled perfusion MRI for clinical applications: A consensus of the ISMRM perfusion study group and the European consortium for ASL in dementia. Magn Reson Med. 2015; 73(1):102–116. [PubMed: 24715426]
36. Buxton RB, Frank LR, Wong EC, Siewert B, Warach S, Edelman RR. A general kinetic model for quantitative perfusion imaging with arterial spin labeling. Magn Reson Med. 1998; 40:383–396. [PubMed: 9727941]
37. Wang J, Alsop DC, Li L, Listerud J, Gonzalez-At JB, Schnall MD, Detre JA. Comparison of quantitative perfusion imaging using arterial spin labeling at 1.5 and 4. 0 Tesla. Magn Reson Med. 2002; 48(2):242–254. [PubMed: 12210932]
38. Lu H, Clingman C, Golay X, van Zijl PC. Determining the longitudinal relaxation time (T1) of blood at 3. 0 Tesla. Magn Reson Med. 2004; 52(3):679–682. [PubMed: 15334591]
39. Ethofer T, Mader I, Seeger U, Helms G, Erb M, Grodd W, Ludolph A, Klose U. Comparison of longitudinal metabolite relaxation times in different regions of the human brain at 1. 5 and 3 Tesla. Magn Reson Med. 2003; 50(6):1296–1301. [PubMed: 14648578]
40. Herscovitch P, Raichle ME. What is the correct value for the brain-blood partition coefficient for water? J Cereb Blood Flow Metab. 1985; 5(1):65–69. [PubMed: 3871783]
41. Ashburner J, Friston KJ. Unified segmentation. Neuroimage. 2005; 26(3):839–851. [PubMed: 15955494]
42. Tzourio-Mazoyer N, Landeau B, Papathanassiou D, Crivello F, Etard O, Delcroix N, Mazoyer B, Joliot M. Automated anatomical labeling of activations in SPM using a macroscopic anatomical parcellation of the MNI MRI single-subject brain. Neuroimage. 2002; 15(1):273–289. [PubMed: 11771995]
43. Snedecor, GW.; Cochran, WG. Statistical methods. Ames, Iowa: Iowa State University; 1967.
44. Howell, DC. Statistical methods for psychology. Belmont, CA: Duxbury; 1997.
45. Pitman EG. A note on normal correlation. Biometrika. 1939; 31:9–12.
46. Borghammer P, Aanerud J, Gjedde A. Data-driven intensity normalization of PET group comparison studies is superior to global mean normalization. Neuroimage. 2009; 46(4):981–988. [PubMed: 19303935]
47. Borghammer P, Jonsdottir KY, Cumming P, Ostergaard K, Vang K, Ashkanian M, Vafaee M, Iversen P, Gjedde A. Normalization in PET group comparison studies--the importance of a valid reference region. Neuroimage. 2008; 40(2):529–540. [PubMed: 18258457]

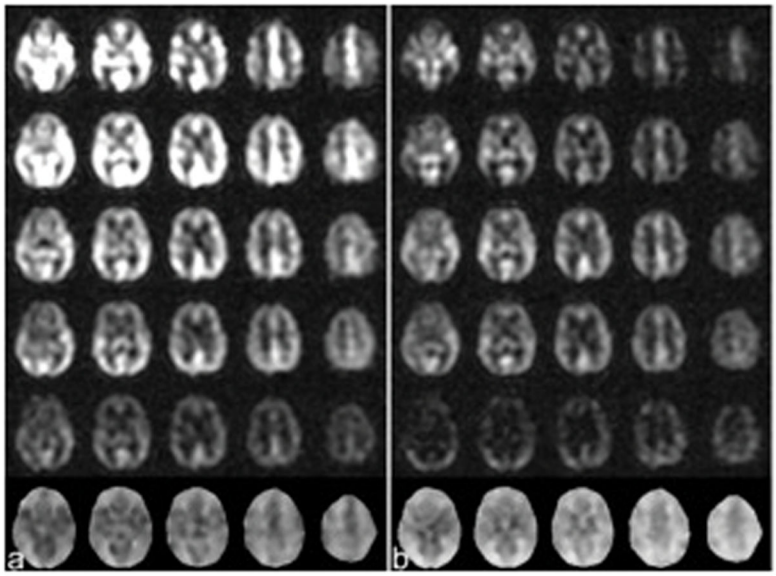

Fig. 1.

The ASL subtraction images of different slices with constant labeling duration of 2.0s but different delays of 0.7, 1.3, 1.9, 2.5 and 3.0s (the first row to the fifth row) and the arterial transit time maps (ATTs) (the sixth row) calculated from the subtraction images of multiple different delay when the images were acquired from an elderly subject (a) without vessel suppression and (b) with vessel suppression.

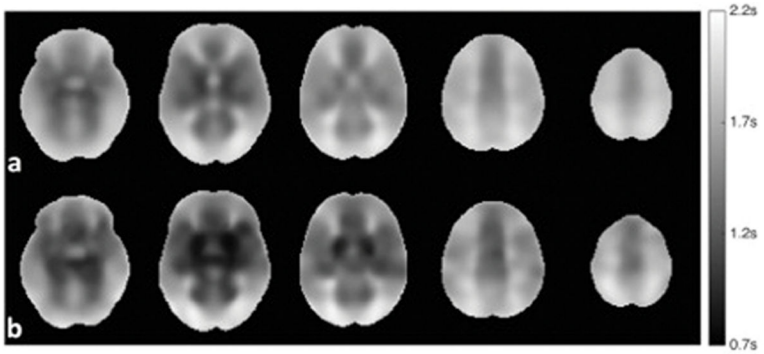

Fig. 2.

Mean vessel-suppressed ATT maps derived from (a) 140 elderly subjects and (b) 9 young subjects. The mean ATT maps were first normalized to the standard MNI space and then averaged over the elderly group and young group respectively.

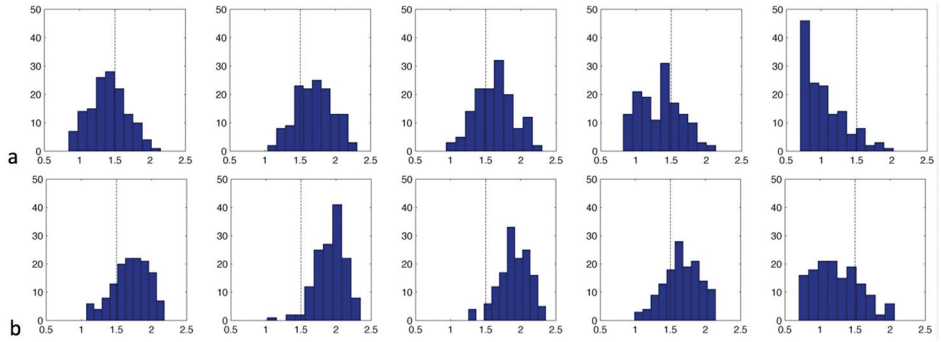

Fig. 3.

Distributions of the arterial transit times (ATTs) (a) without vessel suppression and (b) with vessel suppression in the elderly subjects (n=140) in (from left to right) frontal cortex, occipital cortex, parietal cortex, temporal cortex and basal ganglia. The center of ATTs with vessel suppression in each region shifted to the right compared to without vessel suppression.

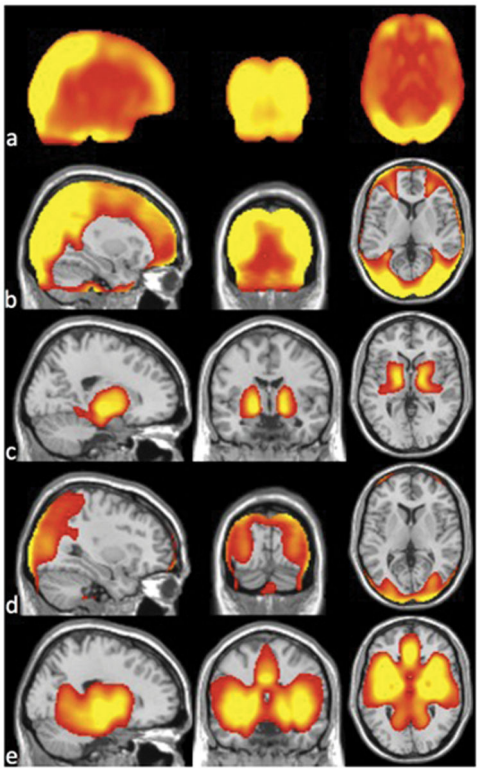

Fig. 4.

(a) Average difference map over the elderly subjects between CBF calculated with ATT correction and without ATT correction and anatomical brain overlaid with the regions where (b) ATT is significantly longer than 1.5 s and (c) ATT is shorter than 1.5 s with vessel suppression, and (d) ATT is longer than 1.5 s without vessel suppression and (e) ATT is shorter than 1.5 s without vessel suppression for the elderly subjects (n=140).

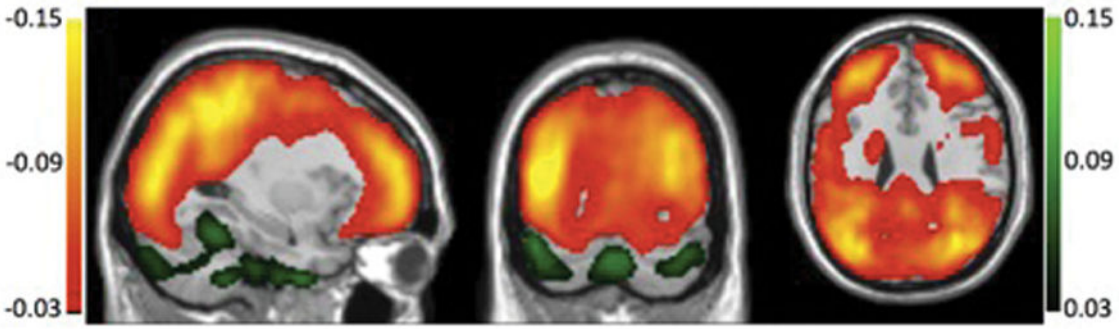

Fig. 5.

Anatomical brain overlaid with the regions where coefficient-of-variation (CV) map of CBF across the elderly subjects (n=140) is reduced (red-yellow color) and increased (green color) with ATT correction compared to without ATT correction as a percentage of the uncorrected CV.

Table 1

Demographics of study population

N=140	
Age in years	
Mean (SD)	76.00 (4.45)
Gender N (%)	
Female	83 (59.3%)
Male	57 (40.7%)
Education in years	
Mean (SD)	14.99 (2.77)
GCP	
Mean (SD)	58.48 (7.17)
Age category N (%)	
70–74	66 (47.1%)
75–79	46 (32.9%)
80 or over	28 (20.0%)

Table 2

Regional arterial transit times of the young (n=9) and elderly subjects (n=140)

ATT (s)	Superior Frontal	Middle Frontal	Inferior Frontal	Superior Temporal	Middle Temporal	Inferior Temporal	Superior Parietal	Inferior Parietal	Superior Occipital	Middle Occipital	Inferior Occipital	Basal Ganglia
Elderly wo. VS	1.51±0.27	1.49±0.26	1.28±0.27	1.14±0.31	1.37±0.32	1.48±0.28	1.73±0.26	1.52±0.31	1.73±0.27	1.76±0.27	1.56±0.32	1.08±0.28
Elderly w. VS	**1.76±0.25**	**1.80±0.25**	**1.58±0.27**	1.47±0.32	1.69±0.27	1.76±0.22	1.96±0.21	1.85±0.25	1.93±0.21	1.99±0.22	1.79±0.25	**1.26±0.35**
Young w. VS	**1.59±0.19**	**1.64±0.18**	**1.35±0.20**	1.33±0.21	1.60±0.17	1.69±0.17	1.92±0.18	1.75±0.18	1.94±0.20	1.99±0.15	1.72±0.25	**0.91±0.20**

*ATT values with Bold face indicate statistical difference between elderly w. VS and young w. VS with threshold of 0.05 using a Mann-Whitney U-test.